THE JOURNAL OF BIOLOGICAL CHEMISTRY VOL. 291, NO. 45, pp. 23793–23803, November 4, 2016

Very Low Density Lipoprotein Assembly Is Required for cAMP-responsive Element-binding Protein H Processing and Hepatic Apolipoprotein A-IV Expression*

Received for publication, July 19, 2016, and in revised form, September 6, 2016 Published, JBC Papers in Press, September 21, 2016, DOI 10.1074/jbc.M116.749283

Dongmei Cheng[‡], Xu Xu[§], Trang Simon[¶], Elena Boudyguina[‡], Zhiyong Deng[‖], Melissa VerHague[‡], Ann-Hwee Lee[§], Gregory S. Shelness[‡], Richard B. Weinberg[¶], and John S. Parks[‡1]**

*From the Departments of [‡]Internal Medicine-Section on Molecular Medicine, [¶]Internal Medicine-Section on Gastroenterology, [‖]Cancer Biology, and **Biochemistry, Wake Forest School of Medicine, Winston-Salem, North Carolina 27157 and the [§]Department of Pathology and Laboratory Medicine, Weill Cornell Medical College, New York, New York 10065*

Edited by George Carman

Hepatic apolipoprotein A-IV (apoA-IV) expression is correlated with hepatic triglyceride (TG) content in mouse models of chronic hepatosteatosis, and steatosis-induced hepatic apoA-IV gene expression is regulated by nuclear transcription factor cAMP-responsive element-binding protein H (CREBH) processing. To define what aspects of TG homeostasis regulate hepatic CREBH processing and apoA-IV gene expression, several mouse models of attenuated VLDL particle assembly were subjected to acute hepatosteatosis induced by an overnight fast or short term ketogenic diet feeding. Compared with chow-fed C57BL/6 mice, fasted or ketogenic diet-fed mice displayed increased hepatic TG content, which was highly correlated (r^2 = 0.95) with apoA-IV gene expression, and secretion of larger, TG-enriched VLDL, despite a lower rate of TG secretion and a similar or reduced rate of apoB100 secretion. When VLDL particle assembly and secretion was inhibited by hepatic shRNA-induced apoB silencing or genetic or pharmacologic reduction in microsomal triglyceride transfer protein (MTP) activity, hepatic TG content increased dramatically; however, CREBH processing and apoA-IV gene expression were attenuated compared with controls. Adenovirus-mediated reconstitution of MTP expression proportionately restored CREBH processing and apoA-IV expression in liver-specific MTP knock-out mice. These results reveal that hepatic TG content, *per se*, does not regulate CREBH processing. Instead, TG mobilization into the endoplasmic reticulum for nascent VLDL particle assembly activates CREBH processing and enhances apoA-IV gene expression in the setting of acute steatosis. We conclude that VLDL assembly and CREBH activation play key roles in the response to hepatic steatosis by up-regulating apoA-IV and promoting assembly and secretion of larger, more TG-enriched VLDL particles.

Over the past decade, the incidence of nonalcoholic fatty liver disease (NAFLD)[2] has reached epidemic levels in developed countries, and it has emerged as a major preventable cause of cirrhosis (1, 2). The central pathophysiology underlying NAFLD is the accumulation of abnormal amounts of triglyceride (TG) within hepatocytes (steatosis), which can initiate inflammation (steatohepatitis) and fibrosis (3). Hepatic TG content is controlled by multiple dietary, hormonal, and genetic factors that regulate the balance among fatty acid uptake, synthesis, oxidation, and export via secretion of TG-rich VLDLs (3, 4). In NAFLD, both TG synthesis and secretion are increased, but TG export is inadequate to prevent steatosis (5, 6). The efficiency of hepatic TG export via the VLDL secretion pathway can be increased by assembly of a greater number of VLDL particles and/or larger VLDL particles that contain more core TG (7, 8). Understanding the mechanisms that integrate VLDL particle number and size to maintain a rate of hepatic TG efflux sufficient to prevent steatosis could provide new insights into the pathogenesis of NAFLD and suggest novel strategies for its prevention and treatment.

One factor that may play an important role in modulating VLDL particle size during TG-rich lipoprotein assembly is apolipoprotein A-IV (apoA-IV). ApoA-IV is a 46-kDa lipid-binding protein, which is expressed in the mammalian intestine and liver (9–12). Although a broad spectrum of functions in lipid metabolism and metabolic regulation has been ascribed to apoA-IV since its discovery in 1977 (9), the largest body of literature has focused on the powerful impact of TG absorption on the induction of intestinal apoA-IV gene expression (13, 14). More recently, Lu *et al.* (15) reported the direct impact of apoA-IV expression on intestinal TG transport efficiency by demonstrating in a transfected cultured pig intestinal epithelial cell line that apoA-IV expression enhances transcellular TG transport, primarily by promoting lipoprotein particle expansion (16). We subsequently observed similar effects in transfected rat hepatoma cells and proposed that apoA-IV alters the

* This work was supported in part by National Institutes of Health Grants R01 HL 119983 (to J. S. P.) and R01 DK089211 (to A. L.). The authors declare that they have no conflicts of interest with the contents of this article. The content is solely the responsibility of the authors and does not necessarily represent the official views of the National Institutes of Health.

[1] To whom correspondence should be addressed: Dept. of Internal Medicine-Section on Molecular Medicine, Wake Forest School of Medicine, Medical Center Blvd., Winston-Salem, NC 27157. Tel.: 336-716-2145; Fax: 336-716-6279; E-mail: jparks@wakehealth.edu.

[2] The abbreviations used are: NAFLD, nonalcoholic fatty liver disease; apo, apolipoprotein; CREBH, cAMP-responsive element-binding protein H; ifu, infectious units; keto, ketogenic; MTP, microsomal triglyceride transfer protein; hMTP, human MTP; MTPLKO, liver-specific MTP knockout; TG, triglyceride; ER, endoplasmic reticulum; Ad-hMTP, adenovirus expressing hMTP; Ad-LacZ, adenovirus expressing LacZ.

trafficking kinetics of nascent apoB-containing lipoproteins by a direct interaction with apoB within the secretory pathway (17, 18). Most recently, we demonstrated *in vivo* that hepatic apoA-IV expression is increased in mouse models of chronic steatosis, is closely correlated with hepatic TG content, and exerts a powerful impact on hepatic lipid content by promoting nascent VLDL particle expansion and TG efflux without increasing the number of atherogenic apoB-containing lipoprotein particles secreted by the liver (19).

Elucidating factors that regulate hepatic apoA-IV expression is relevant to understanding its role in VLDL assembly, TG efflux, and hepatic TG homeostasis. We recently established that hepatosteatosis-induced hepatic apoA-IV gene expression is regulated by the proteolytic processing of the ER-tethered nuclear transcription factor cAMP-responsive element-binding protein H (CREBH) (20). Herein, we investigated hepatic CREBH processing, apoA-IV gene expression, and liver TG content in mouse models of attenuated VLDL particle assembly that were further subjected to perturbations in hepatic lipid content by fasting or by short term feeding of a ketogenic (keto) diet. Our results provide compelling evidence that, in the setting of acute hepatic steatosis, lipid flux across the ER membrane during nascent VLDL particle assembly, rather than bulk hepatic TG content, activates CREBH proteolytic processing, which, in turn, promotes apoA-IV expression. Our data further suggest that CREBH processing and apoA-IV play a coordinated role in promoting the assembly and secretion of larger, TG-enriched VLDL particles, thereby increasing hepatic TG efflux without increasing VLDL particle number.

Results

Hepatic ApoA-IV Expression Is Increased in Models of Acute Steatosis—We previously demonstrated that hepatic apoA-IV expression is increased in several mouse models of chronic and acute steatosis (19, 20). To further explore the basis for the relationship between hepatic TG homeostasis and apoA-IV expression, we examined hepatic apoA-IV gene expression in mice after an overnight fast (20, 21), in mice after short term (6 days) keto diet exposure (20), or in animals provided free access to chow (*i.e.* fed). Previous studies showed that overnight fasting or keto diet increases CREBH processing (20, 22). Plasma TG concentrations were unchanged after an overnight fast compared with fed mice (fasted 48 ± 15 mg/dl *versus* fed 64 ± 4 mg/dl, mean ± S.D., $n = 3$); however, hepatic TG content increased 9.6-fold for fasted mice relative to fed controls (Fig. 1*A*). In comparison, the keto diet significantly raised plasma TG concentrations (91 ± 9 mg/dl, $n = 3$) and increased hepatic TG content 26- and 2.7-fold *versus* chow-fed and fasted mice, respectively (Fig. 1*A*). Quantitative real-time PCR revealed that relative to chow-fed controls, hepatic apoA-IV mRNA abundance increased 8-fold with overnight fasting and 27-fold with keto diet exposure (Fig. 1*B*). Although apoA-IV protein abundance was below the limits of detection for fed and fasted mice, the keto diet-fed mice displayed dramatically increased levels of hepatic apoA-IV (Fig. 1*C*). Plasma apoA-IV was also increased in keto diet-fed mice compared with fed and fasted mice (Fig. 1*D*). Of note, hepatic apoB protein was also increased with fasting and keto diet feeding, relative to fed mice; microsomal triglyceride transfer protein (MTP) abundance was similar for all three groups of mice (Fig. 1*C*). Analysis of individual animal data from both acute steatosis models revealed a strong association between hepatic TG content and apoA-IV mRNA expression (Fig. 1*E*; $r^2 = 0.95$). *In vivo* TG secretion after detergent block of TG lipolysis demonstrated significant ($p < 0.001$) decreases in the TG secretion rate of fasted and keto diet-fed mice compared with chow-fed controls (Fig. 1*F*), probably due to increased shunting of hepatic fatty acids into fatty acid oxidation (23, 24). After the 3-h detergent block experiment, plasma VLDLs were isolated, and particle sizes were measured by dynamic laser light scattering analysis. Despite a lower *in vivo* TG secretion rate compared with fed mice, fasted and keto diet-fed mice had a distribution of VLDL particles that was skewed toward larger sizes, which was particularly exaggerated for keto diet-fed mice (Fig. 1*G*). Aggregating the VLDL particle size data into three broad size ranges revealed that fasted and keto diet-fed mice had significantly fewer VLDL particles in the smallest (<100 nm) size range and more in the 100–200 nm range compared with chow-fed mice (Fig. 1*H*). Moreover, the keto diet-fed mice had significantly more VLDL particles in the largest (>200 nm) size range compared with the other two groups. Secretion of newly synthesized plasma [^{35}S]apoB100 during the Triton block experiment was similar for fed and fasted mice but was significantly ($p < 0.05$) reduced for keto diet-fed mice (Fig. 1*I*).

ApoB Expression Is Essential for Promoting CREBH Processing and Hepatic ApoA-IV Expression—Early studies reported that hepatic apoA-IV expression is regulated by multiple factors, including nutritional and metabolic stress (21), insulin (25), liver X receptors (26), and transcription factors such as LUMAN (27), HNF-4α, and PGC-1α (21). However, recently we demonstrated that CREBH is a major regulator of apoA-IV transcription (20, 22) and is responsible for increasing apoA-IV expression in steatotic conditions via tandem binding sites on the apoA-IV promoter.

To explore whether VLDL assembly and secretion are required for CREBH processing and apoA-IV expression, adenoviruses harboring apoB shRNA (shRNA-apoB) or non-targeting control shRNA (shRNA-NT) were given by retro-orbital injection to keto diet-fed C57BL6 mice. Immunoblot analysis 3 days after injection showed that both hepatic and plasma apoB protein were greatly reduced in the apoB shRNA-treated mice compared with the non-targeting shRNA controls (Fig. 2, *A* and *B*). Quantitative PCR confirmed that this was the consequence of a >95% decrease in hepatic apoB mRNA abundance (data not shown). As expected, the keto diet induced steatosis in the control mice, and apoB silencing resulted in a further doubling of hepatic TG content (Fig. 2*C*). Despite the dramatic increase in hepatic TG accumulation caused by apoB silencing, dramatic reductions in hepatic apoA-IV protein (Fig. 2*D*), mRNA (76% reduction; data not shown), and CREBH processing were observed in mice treated with the higher adenoviral dose of shRNA-apoB (Fig. 2*E*, *mice 135* and *136*). Two additional mice treated with the lower dose of shRNA-apoB (Fig. 2*E*, *mice 133* and *134*) had a less striking reduction in hepatic apoB protein expression and CREBH processing. Neither microsomal CREBH (*i.e.* CREBH full-length (*CREBH (F)*); Fig. 2*E*) nor

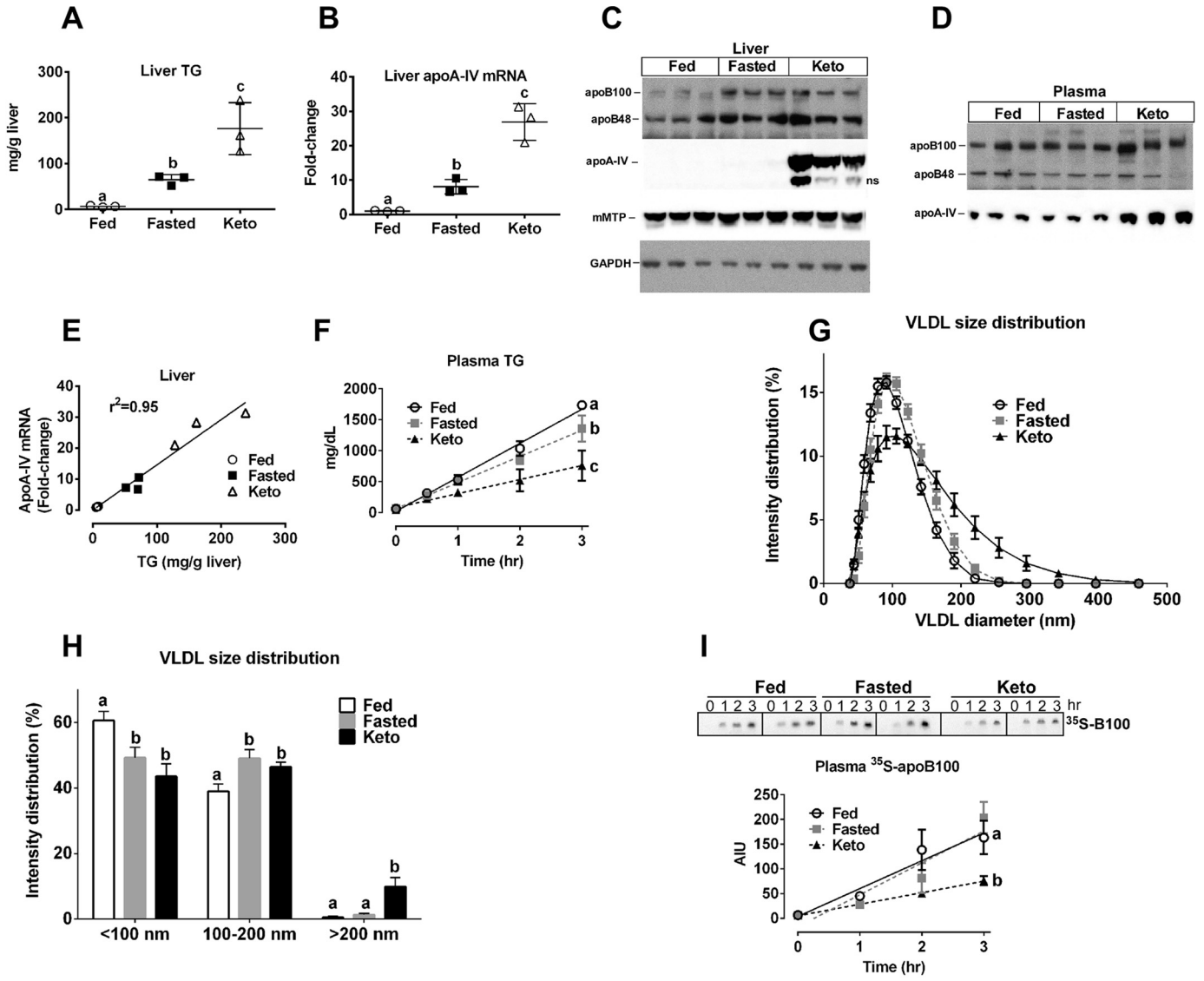

FIGURE 1. **Acute hepatic steatosis induces apolipoprotein A-IV (apoA-IV) expression and secretion of larger VLDL particles.** Chow-fed C57BL6 mice were fasted overnight for 16 h (*Fasted*) or allowed free access to chow (*Fed*); another group of mice was fed a ketogenic diet (*Keto*) for 6 days. Mice were sacrificed between 9 and 10 a.m. Liver TG was measured by an enzymatic assay, and relative mRNA (apoA-IV) and protein levels (apoB, apoA-IV, and MTP) were quantified by real-time PCR and immunoblot analysis, respectively. *A*, liver TG content. *B*, liver apoA-IV mRNA levels normalized to the chow-fed group. *C*, immunoblot of liver apoB, apoA-IV, and MTP. GAPDH was used as a load control. *ns*, nonspecific. *D*, immunoblot of plasma apoB and apoA-IV. *E*, correlation between liver TG content and apoA-IV mRNA abundance. Each *symbol* denotes an individual animal with the line of best fit, determined by linear regression analysis, and coefficient of determination shown for all animals. *A* and *B*, mean ± S.D. (*error bars*); $n = 3$/group. Results are representative of three independent experiments. *F–I*, *in vivo* TG and apoB100 secretion were measured after Triton block of plasma TG lipolysis ($n = 5$ mice/group). *F*, plasma TG secretion rate. Plasma TG concentrations were measured by enzymatic assay at each time point after Triton injection. Data points represent the mean ± S.D. for each time point. The line of best fit, determined by linear regression analysis, is shown for each group. The regression plot slope for each animal was determined; the mean slope for each of the three groups was significantly different (fed, 540 ± 10; fasted, 423 ± 30; keto, 227 ± 36 mg/dl/h), by one-way ANOVA ($p < 0.001$), as denoted by *different letters* on the *plot*. *G*, VLDL particle size distribution. At the termination of the Triton block experiment (3 h time point), mice were euthanized, and a terminal blood sample was taken for VLDL isolation by ultracentrifugation at $d = 1.006$ g/ml. VLDL particle size distribution was measured using dynamic laser light scattering and plotted as percentage intensity distribution. Data points represent the mean ± S.D. for each size range. *H*, binned VLDL particle size distribution. VLDL particle sizes determined in *G* were binned into three size ranges, <100, 100–200, and >200 nm, and plotted as percentage intensity distribution (mean ± S.D.). *Bars* with *different letters* are significantly ($p < 0.03$) different by one-way ANOVA. *I*, secretion rate of newly synthesized plasma [^{35}S]apoB100. Mice were injected with Triton, to block TG hydrolysis, and [^{35}S]Met/Cys. At the indicated time points, blood samples were taken, plasma proteins were fractionated by SDS-PAGE, the apoB100 band was visualized with phosphorimaging analysis, and band intensity was quantified using Multigauge software. Data points (arbitrary intensity units (*AIU*)) represent the mean ± S.E. for each time point ($n = 3–4$). The line of best fit, determined by linear regression analysis, is shown for each group, and slopes for each animal were determined; slopes for the fed (56 ± 14, $n = 3$) and fasted (64 ± 11, $n = 3$) mice were similar, whereas the slope for keto diet-fed animals (23 ± 3, $n = 4$) was significantly ($p < 0.05$) lower, by one-way ANOVA, as denoted by *different letters* on the *plot*. Representative phosphorimaging results for two mice in each group are shown *above* the *plot*.

mRNA abundance (data not shown) was affected by apoB silencing. These data suggest that VLDL particle assembly is necessary for CREBH processing and subsequent up-regulation of apoA-IV gene expression under steatotic conditions.

MTP Is Essential for Promoting CREBH Processing and Hepatic ApoA-IV Expression—VLDL assembly and secretion require MTP (28). To examine the role of MTP protein and activity on steatosis-induced CREBH processing and up-regu-

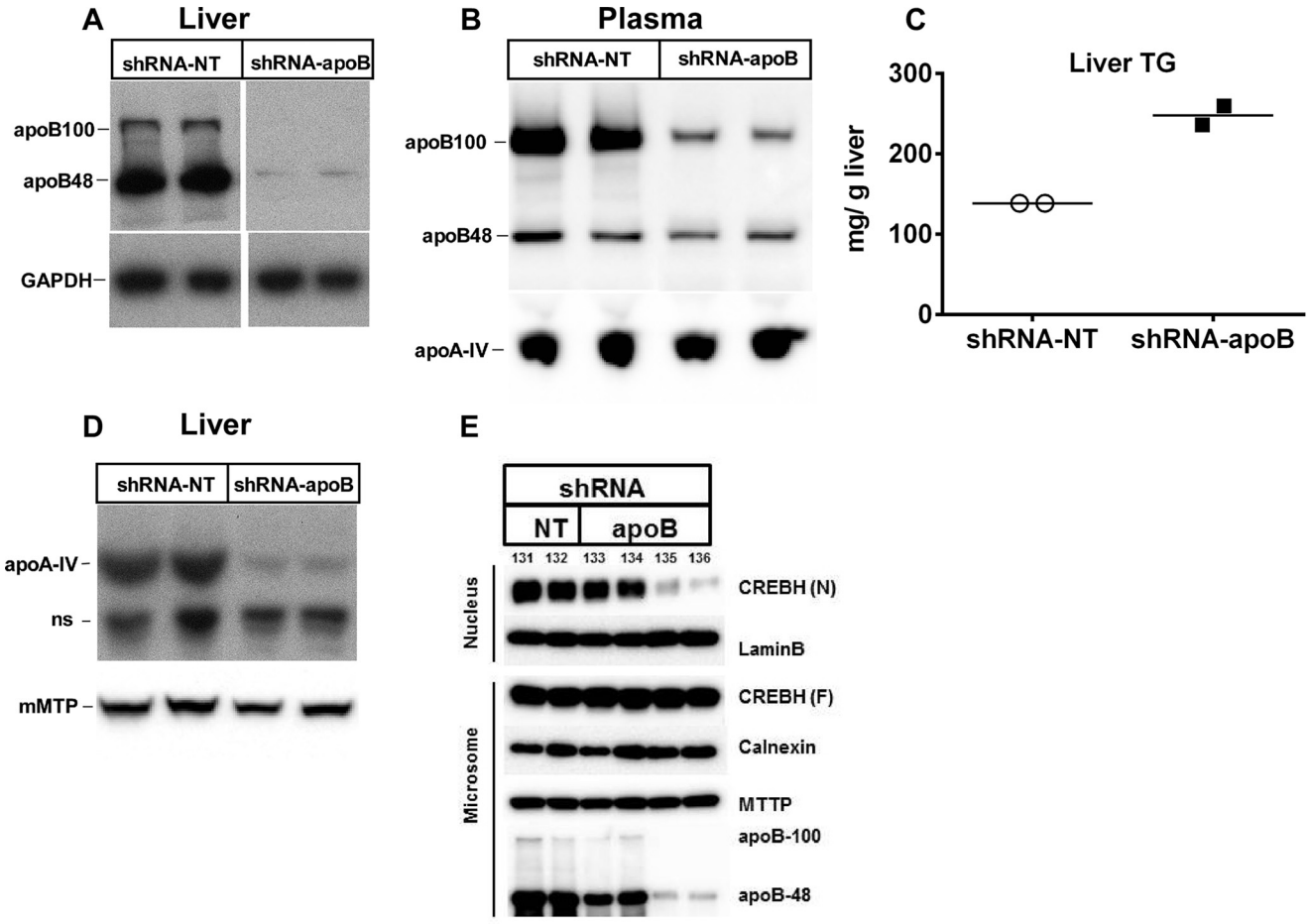

FIGURE 2. **Silencing of hepatic apoB expression induces steatosis and inhibits CREBH processing and hepatic apoA-IV expression.** C57BL6 mice fed a keto diet for 4 days were administered recombinant adenovirus expressing apoB shRNA (shRNA-apoB) or non-targeting control shRNA (shRNA-NT) by retro-orbital injection (for all experiments, 2×10^8 ifu/mouse, except in *E*, where a lower dose, 1×10^8 ifu/mouse, was also given). Three days after adenovirus injection, liver TG was measured by enzymatic assay and relative apoB, apoA-IV, and CREBH mRNA and protein levels were measured by quantitative real-time PCR and immunoblot analysis, respectively. The abundance of full-length, precursor CREBH (*CREBH* (*F*)) and processed, mature CREBH (*CREBH* (*N*)) was determined by immunoblot analysis after isolating hepatic microsomal and nuclear fractions. *A*, liver apoB protein; data are from the same gel, but images have been cropped and placed together. *B*, plasma apoB and apoA-IV protein. *C*, liver TG content; $n = 2$/group. *Horizontal lines* denote *mean*. *D*, liver apoA-IV protein; *ns*, nonspecific. *E*, liver CREBH processing. *Numbers above CREBH* (*N*) identify individual mice. Two additional mice (*133* and *134*) were given a lower dose (1×10^8 ifu/mouse) of apoB shRNA adenovirus and are included in *E* to show the relationship between apoB expression and CREBH processing.

lation of hepatic apoA-IV expression, we generated MTP liver-specific knock-out (MTPLKO) mice to eliminate hepatocyte MTP expression and treated C57BL6 WT mice with an MTP inhibitor (BMS-212122) to reduce MTP activity (29). MTPLKO mice and WT were fasted overnight for 16 h to induce acute hepatosteatosis. Immunoblot analysis confirmed that there was no detectable MTP expression in MTPLKO mouse liver (Fig. 3*A*). The absence of hepatic MTP caused both plasma and hepatic apoB100 (Fig. 3*A*) to fall to undetectable levels and decreased plasma TG levels in both fed and fasted states compared with WT mice (Fig. 3*B*), indicating that hepatic MTP deficiency had blocked VLDL particle assembly and secretion, as anticipated (28, 30). Fasting induced hepatic TG accumulation in both WT and MTPLKO mice, although the magnitude of steatosis was 4-fold greater in MTPLKO mice (Fig. 3*C*). Fasting-induced steatosis increased apoA-IV mRNA expression 16-fold in WT mice relative to fed mice but did not increase apoA-IV gene expression in MTPKO mice (Fig. 3*D*), despite more severe steatosis (Fig. 3*C*). Inhibition of MTP activity with BMS-212122 (*MTPi*) also reduced plasma TG concentrations (Fig. 3*E*), increased hepatic TG content (Fig. 3*F*), and decreased apoA-IV gene expression (Fig. 3*G*), relative to vehicle-treated mice, in a manner similar to the responses seen in fasted MTPLKO *versus* WT mice. MTP protein (Fig. 3*H*) and mRNA abundance (data not shown) were not affected by MTP inhibition; however, as compared with vehicle-treated control mice, CREBH protein processing was suppressed to levels similar to that observed in vehicle-treated MTPLKO mice (Fig. 3*H*). These data strongly support the conclusion that MTP and VLDL particle assembly plays an important role in activating CREBH processing and up-regulation of hepatic apoA-IV expression in steatosis.

Reconstitution of VLDL Assembly/Secretion with MTP Restores CREBH Processing and Hepatic apoA-IV Expression in MTPLKO Mice—To further explore the importance of VLDL assembly for CREBH processing and apoA-IV expression, MTPLKO mice were administered adenovirus expressing human MTP (Ad-hMTP) or LacZ (Ad-LacZ). Three days after infection, mice were fasted overnight to induce steatosis before liver and plasma were harvested. Immunoblot analysis con-

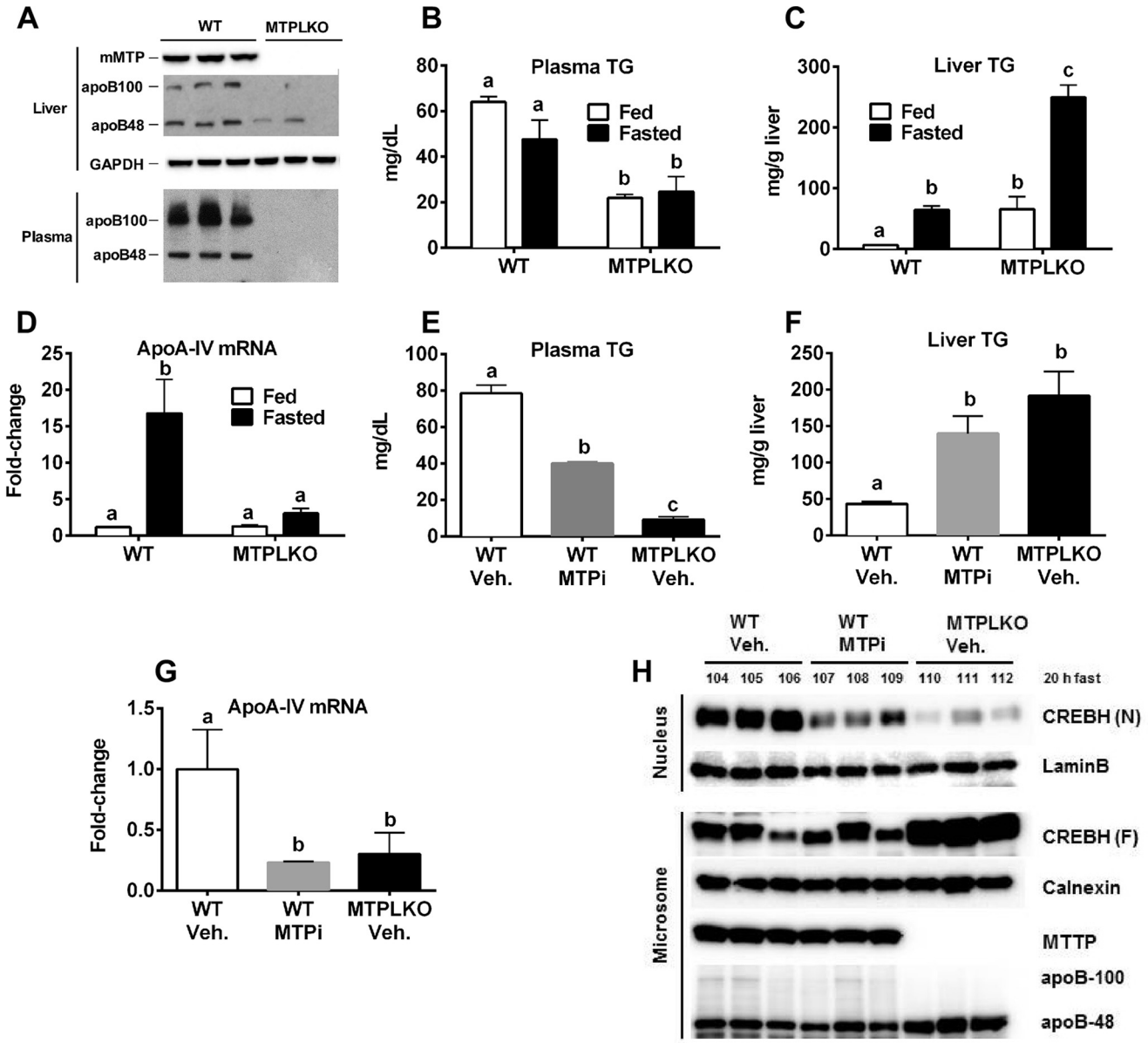

FIGURE 3. **MTP deficiency inhibits CREBH processing and hepatic apoA-IV expression in acute steatosis.** *A–D*, chow-fed MTPLKO and WT mice were either fasted overnight or allowed access to food (*fed*) overnight and then sacrificed. Liver and plasma were collected for measurement of TG, MTP, and apoB protein and apoA-IV mRNA abundance, as described in the legend to Fig. 2. *A*, hepatic MTP and apoB and plasma apoB protein were measured by immunoblot analysis. *B*, plasma TG concentration. *C*, liver TG content. *D*, apoA-IV mRNA levels normalized to chow-fed WT control. *E–H*, chow-fed C57BL6 mice were given either MTP inhibitor BMS212122 (1 mg/mouse/day; *WT-MTPi*) or vehicle (*WT-Veh.*) daily for 2 days by oral gavage; MTPLKO mice were given vehicle (*MTPLKO-Veh.*) as an additional control. All mice were fasted for 20 h to induce acute steatosis, followed by a third dose of MTP inhibitor. Four hours later, mice were sacrificed and liver, and plasma were analyzed as described in the legend to Fig. 2. *E*, plasma TG concentration; *F*, liver TG content; *G*, hepatic apoA-IV mRNA abundance normalized to vehicle-treated WT control; *H*, processing of precursor CREBH (*F*) to mature CREBH (*N*). The *numbers above CREBH* (*N*) identify individual mice. *B–G*, mean ± S.D. (*error bars*), $n = 3$ mice/group. *Bars* with *different letters* in *plots* denote significant difference ($p < 0.05$) by two-way ANOVA (*B–D*) or one-way ANOVA with Tukey's post hoc test (*E–G*).

firmed efficient hepatic hMTP expression in mice injected with Ad-hMTP as well as increased plasma apoB levels, particularly apoB100 (Fig. 4*A*). Plasma TG concentration was significantly increased (Fig. 4*B*), whereas hepatic TG content was significantly reduced (Fig. 4*C*) for Ad-hMTP- *versus* Ad-LacZ-treated mice. As anticipated, quantitative real-time PCR revealed that reconstitution of VLDL assembly with Ad-hMTP did not affect CREBH mRNA abundance (Fig. 4*D*) but restored steatosis-induced CREBH processing (Fig. 4*E*) and apoA-IV gene expression (Fig. 4*F*). Quantitative real-time PCR revealed that the genes encoding other apolipoproteins involved in VLDL synthesis and secretion (*i.e.* apoC-III, apoB, and apoA-V) were unchanged by hMTP reconstitution (Fig. 4*F*), indicating that apoB/MTP-directed VLDL assembly and secretion play a direct and specific role in CREBH processing and apoA-IV expression.

To determine whether hepatic CREBH processing and apoA-IV expression were quantitatively regulated by the level of MTP expression, increasing doses of Ad-hMTP were given to keto diet-fed MTPLKO mice. Quantitative real time PCR and immunoblot analysis demonstrated that hepatic abundance of hMTP mRNA (Fig. 5*A*) and protein (Fig. 5*B*) were

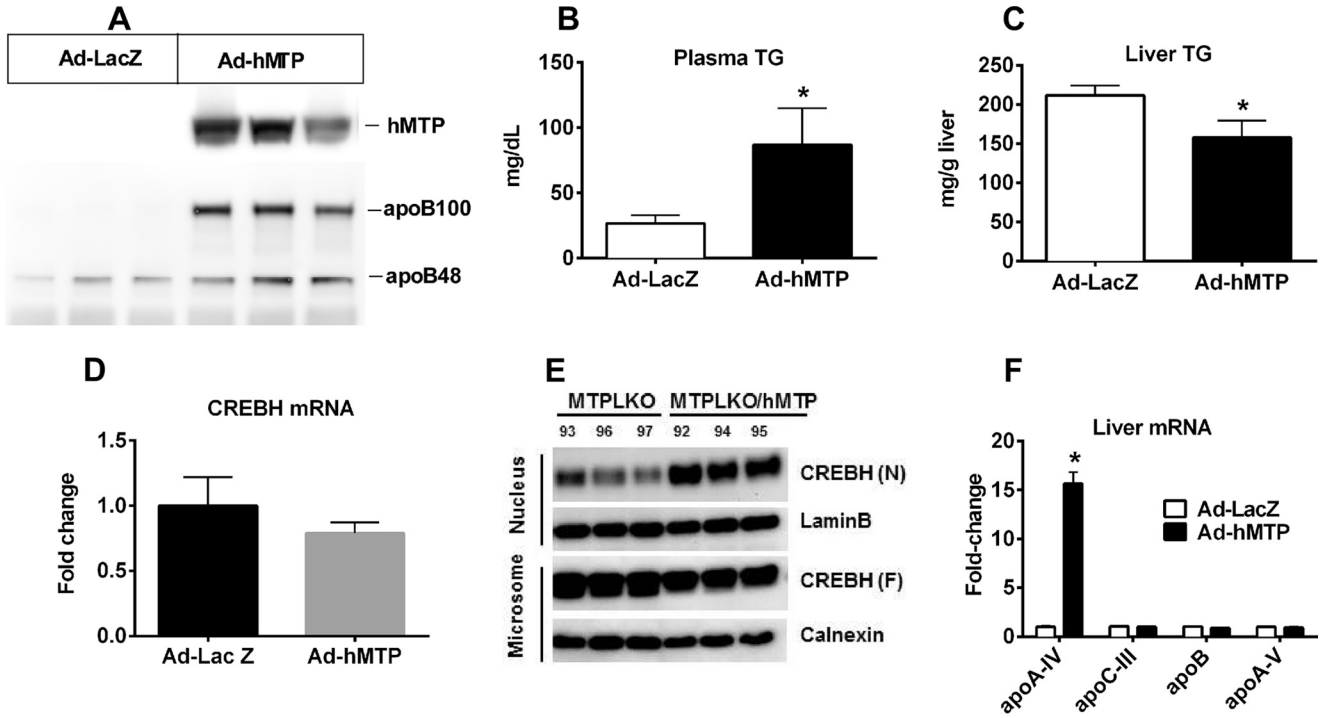

FIGURE 4. **Reconstitution of hepatic MTP expression in chow-fed MTPLKO mice reduces hepatosteatosis and restores CREBH processing and hepatic apoA-IV expression.** MTPLKO mice were given Ad-hMTP or control Ad-LacZ by retro-orbital injection. Three days after adenoviral injection, mice were fasted overnight to induce acute steatosis. Liver and plasma were then harvested to measure hepatic TG content, CREBH processing, and apoA-IV expression, as described in the legend to Fig. 2. *A*, immunoblot of hepatic hMTP expression and plasma apoB protein mass; *B*, plasma TG concentration; *C*, liver TG content; *D*, CREBH mRNA levels normalized to MTPLKO mice given Ad-LacZ; *E*, immunoblot of full-length precursor CREBH (*CREBH* (*F*)) and the processed mature CREBH (*CREBH* (*N*)) in isolated microsomal and nuclear fractions (*numbers above CREBH* (*N*) identify individual mice); *F*, liver mRNA abundance of apoA-IV, apoC-III, apoB, and apoA-V, normalized to MTPLKO mice given Ad-LacZ. *B–D* and *F*, mean ± S.D. (*error bars*), $n = 3$/group. *, $p < 0.05$. Similar results were obtained in a separate experiment using different adenoviral doses.

induced in a dose-dependent manner by Ad-hMTP; control mice (MTPLKO or $Mtp^{flox/flox}$ mice) given the highest dose of Ad-LacZ had no increase in human MTP expression (Fig. 5*A*). Increased hepatic hMTP expression resulted in a trend toward decreased hepatic TG content (Fig. 5*C*) and a proportional increase in plasma apoB100 (Fig. 5*D*), CREBH processing (Fig. 5*E*), and apoA-IV mRNA (Fig. 5*F*) and protein (Fig. 5*G*) abundance. These data suggest that restoration of hepatic MTP in MTPLKO mice proportionately stimulates CREBH processing, apoA-IV expression, and VLDL assembly and secretion.

Discussion

Past studies have shown that hepatic steatosis induces CREBH processing and induction of apoA-IV gene expression (20) and that hepatic apoA-IV overexpression reduces hepatic TG content and increases VLDL TG secretion by promoting an increase in VLDL particle size in a mouse model of chronic steatosis driven by transgenic overexpression of sterol regulatory element-binding protein 1a (SREBP1a) (19). In the current study, we explored more fully the basis for the promotion of CREBH processing and apoA-IV up-regulation and, specifically, whether hepatic TG accumulation, *per se*, promotes CREBH activation or whether processes associated with TG mobilization for nascent VLDL assembly are instead responsible. To distinguish between these possibilities, we investigated hepatic TG content, CREBH processing, and apoA-IV gene expression in mouse models of acute steatosis with intact or disrupted VLDL particle assembly.

Our studies reveal several novel findings. First, using two additional mouse models of acute steatosis, caused by either fasting or feeding a keto diet, we observed a similar relationship between liver TG content and apoA-IV expression as was observed previously using SREBP1a transgenic and high fat diet-fed mice (19). Hence, whether hepatic TG accumulation is induced by enhanced *de novo* lipogenesis, increased dietary fat, or mobilization of adipocyte TG via activated lipolysis, apoA-IV expression is increased via activation of CREBH proteolytic processing. As was observed for SREBP1a transgenic mice (20), increased apoA-IV synthesis was associated with secretion of larger, TG-enriched VLDL particles. Second, attenuation of VLDL particle assembly by apoB silencing or genetic or pharmacologic reduction in MTP activity severely attenuated CREBH processing and apoA-IV expression, despite a dramatic increase in liver TG content. Finally, a direct role of MTP-mediated VLDL assembly in CREBH processing and apoA-IV expression was demonstrated by the fact that MTP reconstitution in MTP-deficient mouse liver with adenoviral expression of human MTP restored both CREBH processing and apoA-IV expression. These studies demonstrate that whereas increasing hepatic TG content is necessary for CREBH-dependent apoA-IV activation, it is not sufficient. Instead, some aspect of the VLDL assembly and secretion pathway is essential for CREBH activation.

Although our current results do not point to which aspect of the VLDL assembly pathway activates CREBH processing, it is

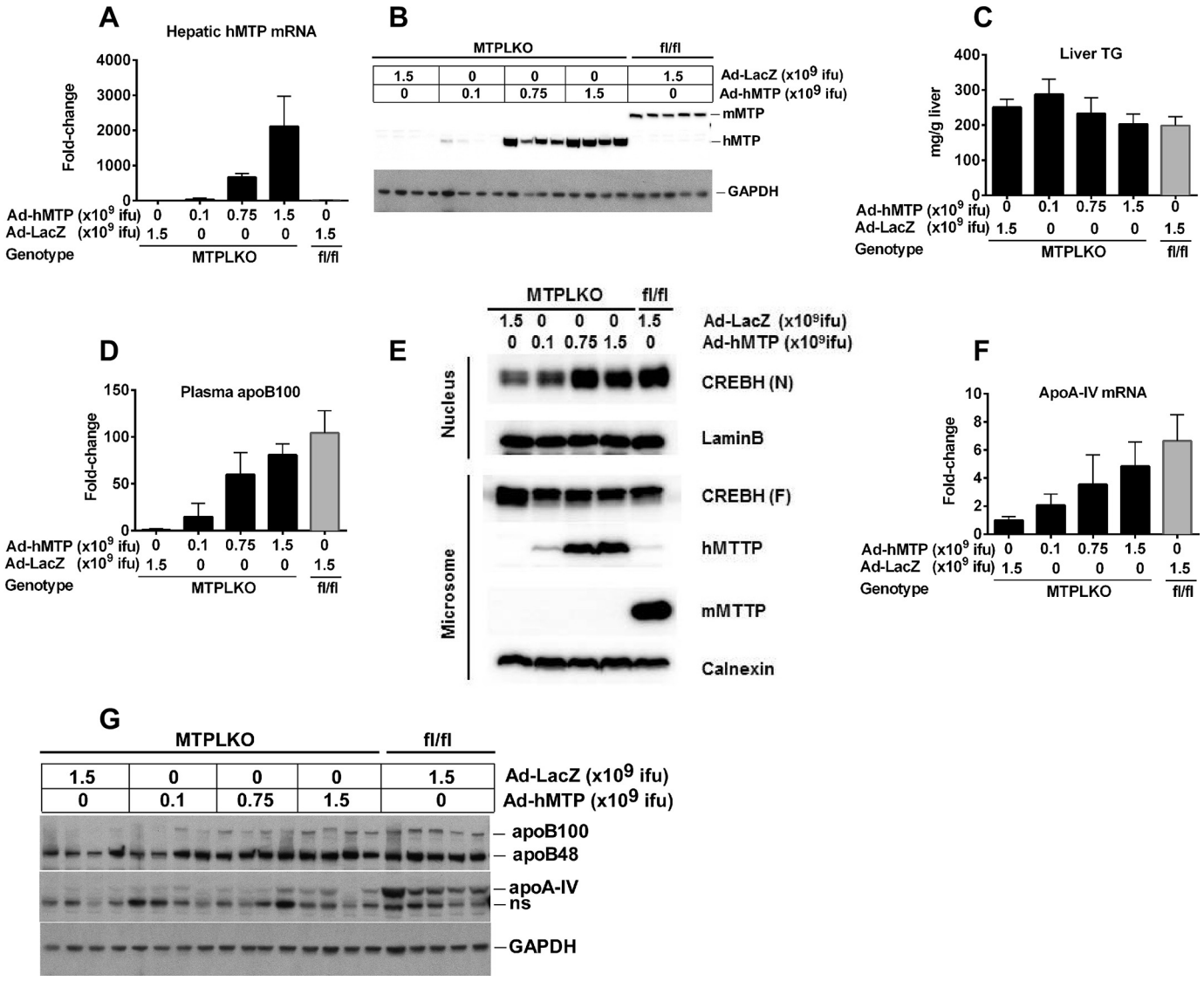

FIGURE 5. **Reconstitution of hepatic CREBH processing and apoA-IV expression is proportional to MTP expression in keto diet-fed MTPLKO mice.** Keto diet-fed MTPLKO mice were given increasing doses of Ad-hMTP (0.1–1.5 × 10^9 ifu) or Ad-LacZ (1.5 × 10^9 ifu) by retro-orbital injection; control littermates (*fl/fl*) were given LacZ adenovirus (1.5 × 10^9 ifu). Three days after adenoviral injection, mice were sacrificed, and liver and plasma were harvested for analyses. *A*, hepatic hMTP mRNA abundance normalized to MTPLKO mice given Ad-LacZ; *B*, hepatic hMTP and mouse MTP (*mMTP*) protein; *C*, hepatic TG content. *D*, plasma apoB protein was detected by immunoblot analysis, quantified using Multigauge software, and normalized to MTPLKO mice given Ad-LacZ. *E*, immunoblot of full-length precursor CREBH (*CREBH* (*F*)) and the processed mature CREBH (*CREBH* (*N*)) in isolated microsomal and nuclear fractions. *F*, hepatic apoA-IV mRNA abundance normalized to MTPLKO mice given Ad-LacZ. *G*, immunoblot of hepatic apoB and apoA-IV protein mass. *ns*, nonspecific. *Error bars*, S.D.

intriguing to note that ER cholesterol content regulates proteolytic activation of SREBP2, another ER-tethered basic helix-loop-helix leucine zipper transcription factor that controls the cellular biosynthesis and uptake of cholesterol (31, 32). Hepatocytes are unique relative to non-lipoprotein-producing cells in that TG synthesis and storage must be coupled to its translocation across the ER membrane to form lumenal lipid droplets, which then serve as a substrate for TG acquisition by apoB (8, 33). Hence, it is intriguing to consider that lipid flux across the ER membrane is required to regulate CREBH cleavage. Previous efforts to dissect the roles of apoB and MTP in VLDL assembly have suggested that MTP is predominantly responsible, perhaps independently of apoB, for the formation of lumenal TG-enriched droplets (34, 35). However, clearly apoB, as the sole TG acceptor in the ER, is also required to maintain ongoing flux of lipid across the ER membrane. Our finding that both apoB and MTP deficiency block CREBH processing suggests that either lipid movement into the ER or some other related function of these proteins initiates the vesicular trafficking of CREBH to the Golgi and processing by site 1 and site 2 proteases to release the active form.

Irrespective of the exact mechanisms, our results reveal a novel pathway in which processes associated with VLDL particle assembly activate CREBH processing, resulting in up-regulation of apoA-IV expression. Since its discovery in 1977 (9), apoA-IV has been reported to have many and varied physiological and metabolic functions (36). Most studies have examined the role of apoA-IV in small intestine physiology, where its expression is robustly up-regulated during lipid absorption (13). We recently explored the role of apoA-IV in hepatic lipid mobilization and demonstrated that steatosis-induced apoA-IV expression enhanced TG secretion and reduced

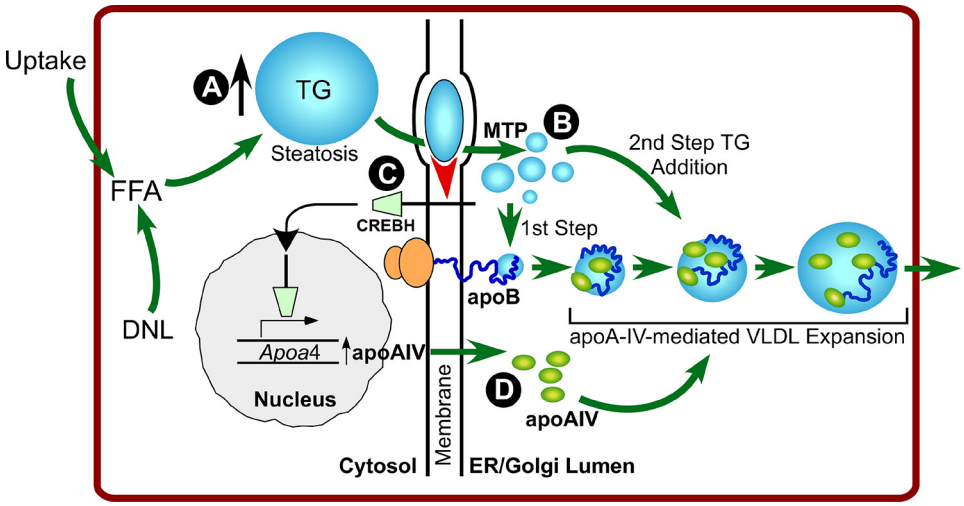

FIGURE 6. **Summary of results and hypothetical model.** Overnight fast and short term keto diet feeding (this study) or dysregulated *de novo* lipogenesis (*DNL*) (19) increases cellular free fatty acid (*FFA*) and esterification to TG, causing steatosis, as evidenced by accumulation of cytosolic TG-enriched lipid droplets (*A*). ApoB lipoprotein assembly requires translocation of TG into and across the ER membrane, a process that requires MTP (*B*). Lumenal lipid is acquired by apoB both during initial, cotranslational TG acquisition (*1st Step*) and during ongoing particle enlargement (*2nd Step*) (8). The ongoing movement of TG across the membrane signals the vesicular transport of CREBH to the Golgi, where it undergoes proteolytic processing (*red arrowhead*; *C*). CREBH activates transcription of apoA-IV, which in turn promotes second step TG addition, most likely by delaying apoB trafficking through the secretory pathway (18) (*D*). The strong relationship between lipid flux across the ER membrane and CREBH processing is supported by data showing that CREBH processing is blocked under conditions of either MTP or apoB inhibition. This pathway provides a compensatory adaptation to hepatic steatosis via the assembly of larger, TG-enriched VLDL particles, which increases TG secretion without increasing the number of atherogenic VLDL particles produced by the liver.

hepatic lipid content by promoting VLDL particle expansion without increasing the number of VLDL particles (19). This pathway probably evolved to increase hepatic TG flux from steatotic liver into the plasma compartment through VLDL particle expansion, thereby protecting the liver from lipid toxicity. Because LDL particle number is more predictive of coronary heart disease than LDL cholesterol (37, 38), the net result of increased hepatic apoA-IV expression would be more efficient hepatic lipid mobilization without increasing secretion of VLDL particles, the precursors of atherogenic plasma LDL particles.

We propose two mechanisms by which apoA-IV may facilitate VLDL particle expansion. The first relates to the interfacial activity and elasticity of apoA-IV, allowing apoA-IV to bind and stabilize the surface monolayer of expanding VLDL particles (39). Second, a direct interaction between apoA-IV and the amino terminus of apoB slows the secretory trafficking of VLDL particles, allowing more lipid addition to the expanding VLDL particle before secretion (18). In the present study, we show that acute steatosis also stimulates apoA-IV expression and secretion of larger VLDL particles, even under metabolic conditions (*i.e.* overnight fasting and keto diet feeding) that lead to an overall reduction in hepatic TG secretion (Fig. 6). This is particularly evident in keto diet-fed mice in which both VLDL TG and apoB100 secretion were reduced compared with chow-fed mice, but plasma VLDL particles were considerably larger and enriched in apoA-IV (data not shown). These results suggest that apoA-IV plays a major role in VLDL particle expansion and in mobilizing TG for secretion to protect the liver from steatosis without increased demand for apoB synthesis.

In addition to increasing hepatic apoA-IV to facilitate VLDL particle expansion, CREBH processing also increases hepatic expression and secretion of apoC-II and apoA-V, both of which activate lipoprotein lipase, increasing lipolysis and clearance of plasma VLDL TG (22). The net result of this CREBH-coordinated physiological response is to shunt TG (*i.e.* fatty acids) out of the liver, through the circulation, and into peripheral tissues. To our knowledge, this is the first evidence for an integrated pathway to protect against hepatosteatosis by exporting excess TG in larger VLDL particles that enter the plasma to undergo stimulated lipolysis with increased fatty acid delivery to peripheral tissues.

ApoA-IV is predominantly expressed in human enterocytes and is highly up-regulated after a fatty meal to facilitate intestinal chylomicron assembly and TG secretion (13, 14). Although human liver apoA-IV mRNA abundance is $<5\%$ of intestinal levels (40, 41), hepatic apoA-IV expression is increased in steatotic states (20), as we have described in mouse models of acute (*i.e.* in the present study) and chronic hepatosteatosis (19). Based on work presented here, we propose that CREBH processing and apoA-IV up-regulation may be an important pathway to facilitate export of excess liver TG in hepatosteatotic individuals.

In summary, we provide evidence for a pathway that integrates increased lipid flux into the ER with increased VLDL particle expansion through activation of CREBH processing, which up-regulates apoA-IV expression. This pathway appears to function in chronic steatosis, induced by high fat diet or genetic induction of lipogenesis, and in acute physiological (overnight fasting) or pathophysiological (ketogenesis) states to protect the liver from lipid overload by promoting TG incorporation into nascent lipoproteins and secretion into the circulation. This integrated lipid transport pathway has dual beneficial purposes, protecting the liver from ectopic lipid accumulation while generating fewer atherogenic plasma apoB lipoprotein particles. Hence, stimulating this pathway would be expected to exert multiple beneficial effects on both fatty liver disease and atherosclerotic cardiovascular disease.

Experimental Procedures

Plasmid Construction

pCMV5-hMTP—hMTP cDNA was obtained by PCR reverse transcription of HuH7 mRNA using primers containing HindIII or XbaI restriction sites (underlined): forward primer, 5′-AGAAAGCTTGCTGGTCAATATGATTCTTCTTGC-3′; reverse primer, 5′-AGATCTAGAATCACAGGTCAGTTTC-AAAACCATCC-3′. The PCR product was cleaved with HindIII and XbaI restriction enzymes, fractionated by agarose gel electrophoresis, and cloned into HindIII/XbaI double-digested pCMV5 expression vector.

pShuttle-hMTP—The pCMV5-hMTP plasmid was linearized with HindIII, blunt ended with T4 DNA polymerase, and then digested with XbaI to release the hMTP cDNA insert. The pShuttle vector (Clontech, catalog no. 631513) was digested with NheI, blunt-ended with T4 DNA polymerase, and then digested with XbaI. The hMTP cDNA was then ligated to pShuttle vector.

pSIREN-apoB shRNA—ApoB shRNA oligonucleotides were synthesized by Integrated DNA Technologies. The oligonucleotide sequences for apoB shRNA are 5′-AATTCAAAAAAGC-AGACAAGCACCTGGAAATTAAGCTTGAATATTTCCA-GGTGCTTGTCTGCG-3′ and 5′-GATCCGCACAACCA-TTTGAGATTACATTCAAGCTTAGTAATCTCAAATGG-TTGTGCTTTTTTG-3′. Non-targeting control shRNA oligonucleotides were from Clontech (catalog no. 631527). The oligonucleotides were annealed to form double-stranded oligonucleotides and inserted into RNAi-Ready pSIREN-Shuttle vector (Clontech, catalog no. 631527). The entire plasmid insert and flanking regions were verified by DNA sequence analysis.

Recombinant Adenovirus Production

The pShuttle gene expression cassettes for human MTP and LacZ (Clontech, catalog no. 631513) and pSIREN-Shuttle vector apoB and control shRNA oligonucleotide-encoding cassettes were released from their respective vectors by restriction enzyme digestion with PI-SceI and I-CeuI and subcloned into the Adeno-X™ expression vector (Clontech, catalog no. 631513), as recommended by the supplier. Recombinant adenoviruses were expanded in HEK293 cells as described in the Adeno-X™ expression system user manual (PT3414-1), purified by cesium chloride gradient ultracentrifugation, dialyzed against dialysis buffer (135 mM NaCl, 1 mM $MgCl_2$, 10 mM Tris-HCl, pH 8.0, 50% glycerol), and stored at −80 °C. Adenovirus titer was measured using the Adeno-X rapid titer kit (Clontech, catalog no. 632250).

Animals

C57BL/6 mice (stock number 000664) were obtained from the Jackson Laboratory. Liver-specific MTP knock-out (MTPLKO) mice were generated by crossing MTP floxed mice ($Mtp^{flox/flox}$), obtained from Dr. Lawrence Chan (Baylor College of Medicine) (28) with albumin *Cre* recombinase-expressing mice (Jackson Laboratory; B6.Cg-Tg(Alb-cre)21Mgn/J). Genotypes were verified by PCR analysis of tail genomic DNA (42). Primers for detecting the loxP site in intron 4 of MTP (28) were 5′-ACAGAGTTATGGAGTTGGAATCAG-3′ and 5′-ATAC-AGCTACTCAGGTCATTGC-3′, and primers for detecting Cre recombinase were 5′-ACCTGAAGATGTTCGCGATT-ATC-3′ and 5′-ACCGTCAGTACGTGAGATATC-3′. Mice homozygous for the MTP floxed allele and harboring a Cre allele were used for studies (*i.e.* MTPLKO). Mice were fed *ad libitum* either a cereal-based rodent chow diet or a keto diet containing 93.4% fat, 4.7% protein, and 1.8% carbohydrate (F-3666, Bio-Serv) for 6 days. All mice were housed in a pathogen-free animal facility in plastic cages in a temperature-controlled room (22 °C) with a 12-h light and 12-h dark cycle. For some experiments, mice were fasted overnight for 16 or 20 h, as indicated, with free access to water. All animal procedures were conducted in conformity with United States Public Health Service policies and were approved by the institutional animal care and use committee of Wake Forest School of Medicine. Mice were deeply anesthetized with ketamine/xylazine before exsanguination via heart puncture. Blood was placed into a tube containing a protease inhibitor mixture (Sigma, catalog no. P2714) dissolved in 0.05% EDTA, 0.05% NaN_3, and plasma was obtained by low speed centrifugation (6000 rpm) for 15 min at 4 °C. Livers were perfused with ice-cold saline and cut into small pieces, snap-frozen in liquid nitrogen, and stored at −80 °C.

Adenoviral Transduction of Mice

Retro-orbital injection of adenovirus was administered under isofluorane sedation. Three days after injection, mice were euthanized, and plasma and liver tissue were harvested as described above.

In Vivo Hepatic TG Secretion

In vivo hepatic TG secretion was measured after detergent block of TG lipolysis, as detailed previously with minor modifications (43). Briefly, mice ($n = 5$/group) were anesthetized and injected in the peritoneal cavity with tyloxapol (Triton WR-1339; 500 mg/kg; Sigma), to block lipolysis, along with [^{3}H]oleate (5 μCi/g body weight) and [^{35}S]Cys/Met (7 μCi/g body weight) as tracers of TG and protein synthesis, respectively. For measurement of the [^{35}S]apoB100 secretion rate, 2 μl of plasma was fractionated by SDS-PAGE, the gel was dried, and the radiolabel in apoB100 was visualized with phosphorimaging and quantified using Multigauge software. VLDL particle size distribution was measured using dynamic laser light scattering as described previously (18).

MTP Inhibitor Study

Chow-fed C57BL6 mice were given either MTP inhibitor BMS212122 (1 mg/mouse/day; a generous gift from Dr. David Gordon, Bristol-Myers Squibb Co., (29)) or vehicle (0.5% carboxymethylcellulose, 2% Tween 80 in water) daily for 2 days by oral gavage; MTPLKO mice were given vehicle as an additional control. All mice were fasted for 20 h to induce acute steatosis, followed by a third dose of MTP inhibitor. Four hours later, mice were sacrificed, and liver and plasma were harvested for analyses.

RNA Extraction and mRNA Quantification

RNA was extracted from frozen liver samples using TRIzol as recommended by the manufacturer (Invitrogen). Total RNA was reverse transcribed into cDNA with random primers using qScript cDNA Supermix (Quanta Biosciences). Quantitative PCR was performed using a 7500 Fast Real-Time PCR System (Applied Biosystems, Foster City, CA). A typical PCR (20 μl) contained 10 μl of 2× Fast SYBR Green Master Mix (Roche Applied Science), 1 μl each of 5 μM forward and reverse primers, and 25 ng of cDNA. Copy numbers were normalized to GAPDH. The following mouse primers were used: forward GAPDH, 5′-TGTGTCCGTCGTGGATCTGA-3′; reverse GAPDH, 5′-CCTGCTTCACCACCTTCTTGAT-3′; forward apoA-IV, 5′-TTCCTGAAGGCTGCGGTGCTG-3′; reverse apoA-IV, 5′-CTGCTGAGTGACATCCGTCTTCTG-3′; forward apoB, 5′-GCTCAACTCAGGTTACCGTGA-3′; reverse apoB, 5′-AGGGTGTACTGGCAAGTTTGG-3′; forward apoA-V, 5′-TCCTCGCAGTGTTCGCAAG-3′; reverse apoA-V, 5′-GAAGCTGCCTTTCAGGTTCTC-3′; forward apoC-III, 5′-TGCTCCAGTAGCCTTTCAGG-3′; reverse apoC-III, 5′-GGTCCAGGATGCGCTAAGTA-3′; forward CREBH, 5′-GGCCATTGACCTGGACATGT-3′; reverse CREBH, 5′-TTCACAGTGAGGTTGAAGCGG-3′. Primers used for human MTP were as follows: forward hMTP, 5′-ACAAGCTCACGTACTCCACTG-3′; reverse hMTP, 5′-TCCTCCATAGTAAGGCCACATC-3′.

Immunoblot Analysis

For immunoblot analysis, ~50 mg of frozen tissue was homogenized with a Polytron homogenizer in lysis buffer (25 mM Tris-HCl, pH 7.4, 300 mM NaCl, and 1% Triton X-100 containing 1 mM PMSF, 10 μg/ml pepstatin, 10 μg/ml leupeptin, and 10 μg/ml aprotinin). Liver protein lysates or plasma were mixed with concentrated SDS-PAGE loading buffer, boiled for 5 min, and then separated by SDS-PAGE. Proteins were electrophoretically transferred to a PVDF membrane, which was then incubated sequentially with primary antibody, HRP-conjugated secondary antibody, and SuperSignal West Pico chemiluminescent substrate (Thermo Scientific, catalog no. 34078). Chemiluminescence was detected by direct visualization with a Fuji LAS3000 Imaging System or with X-film. For the CREBH processing assay, liver nuclear extracts and microsomal fractions were prepared and subjected to immunoblot analysis, as described previously (20). The following primary antibodies were used in this study: rabbit anti-serum raised against purified mouse apoA-IV (19); mouse monoclonal antibody against mouse MTP (BD Transduction Laboratories, catalog no. 612022); rabbit antiserum raised against hMTP (44); goat anti-human apoB (Academy Bio-Medical Co., catalog no. 20A-G1b); and mouse monoclonal antibodies against apoB (45), calnexin (Enzo, catalog no. ADI-SPA-865), LaminB (Santa Cruz Biotechnology, Inc., catalogue no. SC-56145), and CREBH (22).

Analysis of Plasma and Liver Lipids

Plasma TG concentration and liver TG content was quantified using an enzymatic colorimetric assay (Triglycerides/GB kit, Wako) as described previously (46).

Statistical Analysis

Results are presented as means ± S.D., unless otherwise noted. Significance differences in outcome parameters among the different mouse strains and experimental conditions were determined by one-way analysis of variance with Tukey post-hoc analysis.

Author Contributions—D. C. helped design experiments, generated and analyzed data, and wrote the first draft of the manuscript. X. X. performed CREBH processing assays in Figs. 2–5 and analyzed the Western blotting data. T. S. managed mouse colonies and generated the Triton block data in Fig. 1, *F–I*. Z. D. designed shRNA-apoB sequences. M. V. generated some preliminary data. E. B. helped with the mouse sacrifice procedures and Triton block experiments. A.-H. L. and G. S. S. conceived the project, designed experiments, interpreted results, and edited the manuscript. R. B. W. and J. S. P. designed experiments, interpreted results, and edited the manuscript. J. S. P. provided overall supervision for the studies. All authors approved the final version of the manuscript.

Acknowledgment—We gratefully acknowledge and thank Dr. Steve Young (UCLA) for providing monoclonal antibody (2G11) to mouse apoB.

References

1. Cohen, J. C., Horton, J. D., and Hobbs, H. H. (2011) Human fatty liver disease: old questions and new insights. *Science* **332,** 1519–1523
2. Bellentani, S., and Marino, M. (2009) Epidemiology and natural history of non-alcoholic fatty liver disease (NAFLD). *Ann. Hepatol.* **8,** S4–S8
3. Browning, J. D., and Horton, J. D. (2004) Molecular mediators of hepatic steatosis and liver injury. *J. Clin. Invest.* **114,** 147–152
4. Sozio, M. S., Liangpunsakul, S., and Crabb, D. (2010) The role of lipid metabolism in the pathogenesis of alcoholic and nonalcoholic hepatic steatosis. *Semin. Liver Dis.* **30,** 378–390
5. Kawano, Y., and Cohen, D. E. (2013) Mechanisms of hepatic triglyceride accumulation in non-alcoholic fatty liver disease. *J. Gastroenterol.* **48,** 434–441
6. Fabbrini, E., Mohammed, B. S., Magkos, F., Korenblat, K. M., Patterson, B. W., and Klein, S. (2008) Alterations in adipose tissue and hepatic lipid kinetics in obese men and women with nonalcoholic fatty liver disease. *Gastroenterology* **134,** 424–431
7. Fisher, E. A., and Ginsberg, H. N. (2002) Complexity in the secretory pathway: the assembly and secretion of apolipoprotein B-containing lipoproteins. *J. Biol. Chem.* **277,** 17377–17380
8. Shelness, G. S., and Ledford, A. S. (2005) Evolution and mechanism of apolipoprotein B-containing lipoprotein assembly. *Curr. Opin. Lipidol.* **16,** 325–332
9. Swaney, J. B., Braithwaite, F., and Eder, H. A. (1977) Characterization of the apolipoproteins of rat plasma lipoproteins. *Biochemistry* **16,** 271–278
10. Weisgraber, K. H., Bersot, T. P., and Mahley, R. W. (1978) Isolation and characterization of an apoprotein from the d less than 1.006 lipoproteins of human and canine lymph homologous with the rat A-IV apoprotein. *Biochem. Biophys. Res. Commun.* **85,** 287–292
11. Wu, A. L., and Windmueller, H. G. (1978) Identification of circulating apolipoproteins synthesized by rat small intestine *in vivo*. *J. Biol. Chem.* **253,** 2525–2528
12. Green, P. H., Glickman, R. M., Riley, J. W., and Quinet, E. (1980) Human apolipoprotein A-IV: intestinal origin and distribution in plasma. *J. Clin. Invest.* **65,** 911–919
13. Kalogeris, T. J., Rodriguez, M. D., and Tso, P. (1997) Control of synthesis and secretion of intestinal apolipoprotein A-IV by lipid. *J. Nutr.* **127,** 537S–543S.
14. Black, D. D. (2007) Development and physiological regulation of intestinal lipid absorption. I. Development of intestinal lipid absorption: cellular

events in chylomicron assembly and secretion. *Am. J. Physiol. Gastrointest. Liver Physiol.* **293,** G519–G524
15. Lu, S., Yao, Y., Meng, S., Cheng, X., and Black, D. D. (2002) Overexpression of apolipoprotein A-IV enhances lipid transport in newborn swine intestinal epithelial cells. *J. Biol. Chem.* **277,** 31929–31937
16. Lu, S., Yao, Y., Cheng, X., Mitchell, S., Leng, S., Meng, S., Gallagher, J. W., Shelness, G. S., Morris, G. S., Mahan, J., Frase, S., Mansbach, C. M., Weinberg, R. B., and Black, D. D. (2006) Overexpression of apolipoprotein A-IV enhances lipid secretion in IPEC-1 cells by increasing chylomicron size. *J. Biol. Chem.* **281,** 3473–3483
17. Gallagher, J. W., Weinberg, R. B., and Shelness, G. S. (2004) apoA-IV tagged with the ER retention signal KDEL perturbs the intracellular trafficking and secretion of apoB. *J. Lipid Res.* **45,** 1826–1834
18. Weinberg, R. B., Gallagher, J. W., Fabritius, M. A., and Shelness, G. S. (2012) ApoA-IV modulates the secretory trafficking of apoB and the size of triglyceride-rich lipoproteins. *J. Lipid Res.* **53,** 736–743
19. VerHague, M. A., Cheng, D., Weinberg, R. B., and Shelness, G. S. (2013) Apolipoprotein A-IV expression in mouse liver enhances triglyceride secretion and reduces hepatic lipid content by promoting very low density lipoprotein particle expansion. *Arterioscler. Thromb. Vasc. Biol.* **33,** 2501–2508
20. Xu, X., Park, J. G., So, J. S., Hur, K. Y., and Lee, A. H. (2014) Transcriptional regulation of apolipoprotein A-IV by the transcription factor CREBH. *J. Lipid Res.* **55,** 850–859
21. Hanniman, E. A., Lambert, G., Inoue, Y., Gonzalez, F. J., and Sinal, C. J. (2006) Apolipoprotein A-IV is regulated by nutritional and metabolic stress: involvement of glucocorticoids, HNF-4α, and PGC-1α. *J. Lipid Res.* **47,** 2503–2514
22. Lee, J. H., Giannikopoulos, P., Duncan, S. A., Wang, J., Johansen, C. T., Brown, J. D., Plutzky, J., Hegele, R. A., Glimcher, L. H., and Lee, A.-H. (2011) The transcription factor cyclic AMP-responsive element-binding protein H regulates triglyceride metabolism. *Nat. Med.* **17,** 812–815
23. Garbow, J. R., Doherty, J. M., Schugar, R. C., Travers, S., Weber, M. L., Wentz, A. E., Ezenwajiaku, N., Cotter, D. G., Brunt, E. M., and Crawford, P. A. (2011) Hepatic steatosis, inflammation, and ER stress in mice maintained long term on a very low-carbohydrate ketogenic diet. *Am. J. Physiol. Gastrointest. Liver Physiol.* **300,** G956–G967
24. Badman, M. K., Pissios, P., Kennedy, A. R., Koukos, G., Flier, J. S., and Maratos-Flier, E. (2007) Hepatic fibroblast growth factor 21 is regulated by PPARα and is a key mediator of hepatic lipid metabolism in ketotic states. *Cell Metab.* **5,** 426–437
25. Evert, M., Schneider-Stock, R., and Dombrowski, F. (2003) Apolipoprotein A-IV mRNA overexpression in early preneoplastic hepatic foci induced by low-number pancreatic islet transplants in streptozotocin-diabetic rats. *Pathol. Res. Pract.* **199,** 373–379
26. Liang, Y., Jiang, X. C., Liu, R., Liang, G., Beyer, T. P., Gao, H., Ryan, T. P., Dan Li, S., Eacho, P. I., and Cao, G. (2004) Liver X receptors (LXRs) regulate apolipoprotein AIV: implications of the antiatherosclerotic effect of LXR agonists. *Mol. Endocrinol.* **18,** 2000–2010
27. Sanecka, A., Ansems, M., van Hout-Kuijer, M. A., Looman, M. W., Prosser, A. C., Welten, S., Gilissen, C., Sama, I. E., Huynen, M. A., Veltman, J. A., Jansen, B. J., Eleveld-Trancikova, D., and Adema, G. J. (2012) Analysis of genes regulated by the transcription factor LUMAN identifies ApoA4 as a target gene in dendritic cells. *Mol. Immunol.* **50,** 66–73
28. Chang, B. H., Liao, W., Li, L., Nakamuta, M., Mack, D., and Chan, L. (1999) Liver-specific inactivation of the abetalipoproteinemia gene completely abrogates very low density lipoprotein/low density lipoprotein production in a viable conditional knockout mouse. *J. Biol. Chem.* **274,** 6051–6055
29. Robl, J. A., Sulsky, R., Sun, C. Q., Simpkins, L. M., Wang, T., Dickson, J. K., Jr., Chen, Y., Magnin, D. R., Taunk, P., Slusarchyk, W. A., Biller, S. A., Lan, S. J., Connolly, F., Kunselman, L. K., Sabrah, T., *et al.* (2001) A novel series of highly potent benzimidazole-based microsomal triglyceride transfer protein inhibitors. *J. Med. Chem.* **44,** 851–856
30. Raabe, M., Véniant, M. M., Sullivan, M. A., Zlot, C. H., Björkegren, J., Nielsen, L. B., Wong, J. S., Hamilton, R. L., and Young, S. G. (1999) Analysis of the role of microsomal triglyceride transfer protein in the liver of tissue-specific knockout mice. *J. Clin. Invest.* **103,** 1287–1298
31. Radhakrishnan, A., Goldstein, J. L., McDonald, J. G., and Brown, M. S. (2008) Switch-like control of SREBP-2 transport triggered by small changes in ER cholesterol: a delicate balance. *Cell Metab.* **8,** 512–521
32. Das, A., Brown, M. S., Anderson, D. D., Goldstein, J. L., and Radhakrishnan, A. (2014) Three pools of plasma membrane cholesterol and their relation to cholesterol homeostasis. *eLife* 10.7554/eLife.02882
33. Sundaram, M., and Yao, Z. (2010) Recent progress in understanding protein and lipid factors affecting hepatic VLDL assembly and secretion. *Nutr. Metab.* **7,** 35
34. Wang, Y., Tran, K., and Yao, Z. (1999) The activity of microsomal triglyceride transfer protein is essential for accumulation of triglyceride within microsomes in McA-RH7777 cells: a unified model for the assembly of very low density lipoproteins. *J. Biol. Chem.* **274,** 27793–27800
35. Hamilton, R. L., Wong, J. S., Cham, C. M., Nielsen, L. B., and Young, S. G. (1998) Chylomicron-sized lipid particles are formed in the setting of apolipoprotein B deficiency. *J. Lipid Res.* **39,** 1543–1557
36. Wang, F., Kohan, A. B., Lo, C. M., Liu, M., Howles, P., and Tso, P. (2015) Apolipoprotein A-IV: a protein intimately involved in metabolism. *J. Lipid Res.* **56,** 1403–1418
37. Otvos, J. D., Mora, S., Shalaurova, I., Greenland, P., Mackey, R. H., and Goff, D. C., Jr. (2011) Clinical implications of discordance between low-density lipoprotein cholesterol and particle number. *J. Clin. Lipidol.* **5,** 105–113
38. Cromwell, W. C., Otvos, J. D., Keyes, M. J., Pencina, M. J., Sullivan, L., Vasan, R. S., Wilson, P. W., and D'Agostino, R. B. (2007) LDL particle number and risk of future cardiovascular disease in the Framingham offspring study: implications for LDL management. *J. Clin. Lipidol.* **1,** 583–592
39. Weinberg, R. B., Cook, V. R., DeLozier, J. A., and Shelness, G. S. (2000) Dynamic interfacial properties of human apolipoproteins A-IV and B-17 at the air/water and oil/water interface. *J. Lipid Res.* **41,** 1419–1427
40. Elshourbagy, N. A., Walker, D. W., Boguski, M. S., Gordon, J. I., and Taylor, J. M. (1986) The nucleotide and derived amino acid sequence of human apolipoprotein A-IV mRNA and the close linkage of its gene to the genes of apolipoproteins A-I and C-III. *J. Biol. Chem.* **261,** 1998–2002
41. Karathanasis, S. K., Yunis, I., and Zannis, V. I. (1986) Structure, evolution, and tissue-specific synthesis of human apolipoprotein AIV. *Biochemistry* **25,** 3962–3970
42. Timmins, J. M., Lee, J. Y., Boudyguina, E., Kluckman, K. D., Brunham, L. R., Mulya, A., Gebre, A. K., Coutinho, J. M., Colvin, P. L., Smith, T. L., Hayden, M. R., Maeda, N., and Parks, J. S. (2005) Targeted inactivation of hepatic Abca1 causes profound hypoalphalipoproteinemia and kidney hypercatabolism of apoA-I. *J. Clin. Invest.* **115,** 1333–1342
43. Chung, S., Timmins, J. M., Duong, M., Degirolamo, C., Rong, S., Sawyer, J. K., Singaraja, R. R., Hayden, M. R., Maeda, N., Rudel, L. L., Shelness, G. S., and Parks, J. S. (2010) Targeted deletion of hepatocyte ABCA1 leads to very low density lipoprotein triglyceride overproduction and low density lipoprotein hypercatabolism. *J. Biol. Chem.* **285,** 12197–12209
44. Cheng, D., MacArthur, P. S., Rong, S., Parks, J. S., and Shelness, G. S. (2010) Alternative splicing attenuates transgenic expression directed by the apolipoprotein E promoter-enhancer based expression vector pLIV11. *J. Lipid Res.* **51,** 849–855
45. Nguyen, A. T., Braschi, S., Geoffrion, M., Fong, L. G., Crooke, R. M., Graham, M. J., Young, S. G., and Milne, R. (2006) A mouse monoclonal antibody specific for mouse apoB48 and apoB100 produced by immunizing "apoB39-only" mice with mouse apoB48. *Biochim. Biophys. Acta* **1761,** 182–185
46. Carr, T. P., Andresen, C. J., and Rudel, L. L. (1993) Enzymatic determination of triglyceride, free cholesterol, and total cholesterol in tissue lipid extracts. *Clin. Biochem.* **26,** 39–42